11th World Congress on Computational Mechanics (WCCM XI)
5th European Conference on Computational Mechanics (ECCM V)
6th European Conference on Computational Fluid Dynamics (ECFD VI)
E. Oñate, J. Oliver and A. Huerta (Eds)

# A NONLINEAR FINITE ELEMENT FOR SIMULATION OF DYNAMICS OF BEAM STRUCTURES USING MULTIBODY SYSTEM APPROACH

**OLEG DMITROCHENKO[*], GENNADY MIKHEEV[*], DMITRY POGORELOV[*], RAJU GANDIKOTA[†]**

[*]Bryansk State Technical University, Laboratory of Computational Mechanics,
B. 50 let Oktyabrya 7, 241035 Bryansk, Russia, [dmitrochenko, mikheev, pogorelov]@umlab.ru, www.umlab.ru

[†] Weatherford International, 6610 W Sam Houston Pkwy N, Ste 350, TX, U.S.A.,
raju.gandikota@weatherford.com, www.weatherford.com

**Key Words:** *Drilling modeling, Flexible multibody system dynamics, Beam finite elements.*

**Abstract.** Many engineering dynamic problems can be simulated as beam structures. For example, such models are applied in well drilling. Dynamic simulation allows optimizing shape of well bore and operations parameters of the drilling. Calculation speed of simulation of dynamics of a drill string depends on size of matrices of a model and on effectiveness of numerical methods.

The approach to simulation of dynamics of drill strings are suggested by the authors in [1]. The drill string is presented as a set of uniform beams connected via force elements. Flexibility of the beams is simulated using the modal approach. Thus, each beam has at least twelve degrees of freedom: six coordinates define position and orientation of a local frame and six modes are used for modeling flexibility. For simulation of the drilling processes, implicit Park method with Jacobian of stiff forces is used [2]. Analysis of vibration, rock cutting, buckling and post-buckling behaviour and other processes of the drilling can be successfully modeled using the approach. But it has some disadvantages.

Firstly, number of degrees of freedom can be decreased if a single nonlinear finite element model is used instead of the model including great number of beam subsystems. Secondly, simulation of real rotation of the drill string using the modal approach related to the problem with calculation of Jacobians from stiff force elements. The expressions of the modal coordinate derivatives of the stiff forces are variable since each mode is calculated in the local frame of the beam and rotate together with the frame.

## 1 INTRODUCTION

Many engineering dynamic problems can be simulated as beam structures. For example, such models are applied in well drilling. Dynamic simulation allows optimizing shape of well bore and operation parameters of the drilling. Several types of analysis are used for these purposes on the stage of drilling planning. One of them is the torque and drag analysis.

Drill strings can be up to several kilometers long. Dynamic simulation of long drill strings might face to several problems. One of the problems is large number of degrees of freedom in the models. The second one is stiff equations of motion that require special integration methods. For calculating very long drill strings, static equations of so called soft-string models ignoring bending stiffness are commonly used. Such models give accurate results for axial loads and torque if the drill string does not buckle. However it cannot compute contact forces between the drill string and wellbore, cannot simulate buckling and real rotation of the drill string.

If the dynamic simulation is applied, torque and drag analysis of a drill string is reduced to determining the equilibrium conditions under given loads. A small value of kinetic energy of the drill string is the criterion to finish the integration of the equations of motion.

Forced frequency analysis of a bottom hole assembly (BHA) of the drill string placed in the wellbore is another type of analysis applied in drilling. It is carried out to detect drill string rotation rates that can result in BHA resonance vibrations and hits of BHA on wellbore walls. Simplified models of real excitations acting on an assembly are used to catch critical effects of BHA motion.

Calculation efficiency speed of dynamic simulation of a drill string depends on the size of matrices in the model and on efficiency of numerical methods. In this paper, two approaches using the methods of multibody system dynamics for simulation of drill strings arementioned but the detailed derivation is given for the nonlinear finite element approach, see below.

In accordance with the first approach, the component mode synthesis method is applied for modelling of flexibility of beam structures. Its main ideas and some obtained simulation results are presented in [1]. For simulation of drilling processes, implicit Park method with computing Jacobians of stiff forces is used [2]. Parallel computations are implemented for increasing the solver efficiency. Analysis of vibration, rock cutting, buckling and post-buckling behavior and other processes of the drilling can be successfully modeled using the approach. However it has some disadvantages. Firstly, number of degrees of freedom could be decreased if a single nonlinear finite element model were used instead of the model including great number of beams. Secondly, simulation of real rotation of the drill string using the modal approach is related to costly calculation of Jacobians. The expressions for the modal coordinate derivatives of the stiff forces are variable since each mode is calculated in the local frame of the beam and rotates together with the frame.

The second suggested approach is the dynamic simulation of drill strings using nonlinear finite element models. It is considered in the paper in details. Besides decreasing the number of degrees of freedom, buckling is simulated by single finite element with nonlinear stiffness matrices more accuracy as compared with a single beam using modal approach.

All mathematical models and algorithms considered in the paper are implemented in the specialized software developed on the base of «Universal Mechanism» (UM) software [3].

## 2 EQUATION OF MOTION OF BEAM STRUCTURE CREATED BY NONLINEAR FINITE ELEMENT METOD

An efficient approach used for numerical simulation of flexible structures is the floating frame of reference formulation [5]. It allows taking into account the arbitrary spatial motion of the origin of the reference frame rigidly connected with the deformable body. Thus, the approach employs all local flexible degrees of freedom of the structure, and just adds six more degrees of freedom of the floating frame. The limitation of this approach is inherited from the linear equations of motion of the structure within the floating frame.

The extension of this approach is presented in the large rotation vector formulation [6]. In this approach, the floating reference frame is placed to each node of the finite-element mesh of the flexible structure, and the intermediate auxiliary local frame is introduced between the nodes to account for flexibility in local reference frame.

In this research, the latter approach was modified by reducing one node in the local reference frame and keeping only the rest single node to represent the flexibility of the beam, Figure 1. The vector of generalized coordinates of the element has the following form:

$$\mathbf{q} = \{\mathbf{r}_1^{\mathrm{T}} \quad \boldsymbol{\varphi}_1^{\mathrm{T}} \quad \mathbf{r}_2^{\mathrm{T}} \quad \boldsymbol{\varphi}_2^{\mathrm{T}}\}^{\mathrm{T}}, \tag{1}$$

where $\mathbf{r}_1$ and $\mathbf{r}_2$ are the absolute position vectors of the two nodes, while $\boldsymbol{\varphi}_1$ and $\boldsymbol{\varphi}_2$ are the vectors of the orientation angles (Cardan angles are used here: $\boldsymbol{\varphi}_i = \{\alpha_i \quad \beta_i \quad \gamma_i\}^{\mathrm{T}}$) for the nodal cross sections. Also, the dependent local coordinates $\mathbf{u}$ are introduced to represent small displacements of the right-hand-side cross section relative to the left-hand-side one:

$$\mathbf{u}(\mathbf{q}) = \begin{Bmatrix} \{u_1 \;\; u_2 \;\; u_3\}^{\mathrm{T}} \\ \{\alpha_1 \;\; \alpha_2 \;\; \alpha_3\}^{\mathrm{T}} \end{Bmatrix} = \begin{Bmatrix} \mathbf{A}_1^{\mathrm{T}}\{\mathbf{r}_2 - \mathbf{r}_1\} - \{L \;\; 0 \;\; 0\}^{\mathrm{T}} \\ \boldsymbol{\alpha}(\mathbf{A}_1^{\mathrm{T}}\mathbf{A}_2) \end{Bmatrix}, \tag{2}$$

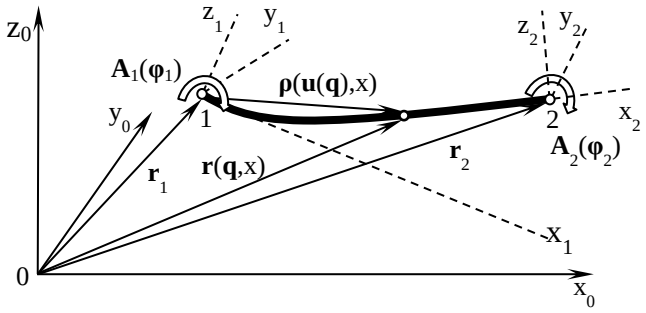


Figure 3. Geometry and generalized coordinates of a single nonlinear beam element.

$\mathbf{A}_1$ and $\mathbf{A}_2$ are matrices of orientation of the nodal cross-sections, Eq. (16), and $\boldsymbol{\alpha}(\mathbf{A})$ is the vector-valued function of a matrix argument, which returns the Cardan angles, given the orientation matrix $\mathbf{A}$; $\alpha_1 = (A_{23} - A_{32})/2$, *etc*. This allows introducing local displacement field $\boldsymbol{\rho}(\mathbf{u}(\mathbf{q}),x)$ of the beam by employing local shape function matrix $\mathbf{N}(x)$:

$$\boldsymbol{\rho}(\mathbf{u}(\mathbf{q}), x) = \mathbf{N}(x)\,\mathbf{u}(\mathbf{q}) + \{x \;\; 0 \;\; 0\}^{\mathrm{T}}, \tag{3}$$

$$\mathbf{N}(x)=\begin{bmatrix} \xi & 0 & 0 & 0 & 0 & 0 \\ 0 & 3\xi^2-2\xi^3 & 0 & 0 & 0 & L(\xi^3-\xi^2) \\ 0 & 0 & 3\xi^2-2\xi^3 & 0 & -L(\xi^3-\xi^2) & 0 \end{bmatrix},\ \xi = \frac{x}{L}.$$

The absolute position of an arbitrary point relative to the fixed frame is computed as follows:

$$\mathbf{r}(\mathbf{q},x)=\mathbf{r}_1+\mathbf{A}_1\,\boldsymbol{\rho}(\mathbf{u}(\mathbf{q}),x)\,. \tag{4}$$

The equations of motion are formulated based on Lagrange equations of the second kind:

$$\frac{\mathrm{d}}{\mathrm{d}t}\frac{\partial T}{\partial \dot{\mathbf{q}}}-\frac{\partial T}{\partial \mathbf{q}}+\frac{\partial \Pi}{\partial \mathbf{q}}=\frac{\partial W}{\partial \mathbf{q}}. \tag{5}$$

Here, $T$ is expression for kinetic energy of the beam element, which is computed as follows:

$$T(\dot{\mathbf{q}},\mathbf{q})=\tfrac{1}{2}\int_0^L \mu\,\dot{\mathbf{r}}^{\mathrm{T}}\dot{\mathbf{r}}\,dx+\tfrac{1}{2}\sum_{k=1}^{2}\boldsymbol{\omega}_k^{\mathrm{T}}\mathbf{J}_{\mathrm{k}}^{\mathrm{t}}\boldsymbol{\omega}_k \tag{6}$$

In Eq. (6), the energy of translational motion of the beam is computed in a consistent way, while the rotational energy is approximately computed in a lumped manner, when the whole rotational inertia is concentrated at the two nodes of the beam, given by tensors of inertia $\mathbf{J}^{\mathrm{t}}_k$. This allows avoiding difficulties of interpolation of 3D rotations along the beam centerline.

The elastic strain energy $\Pi$ in Eq. (5) is computed in terms of local displacements $\mathbf{u}(\mathbf{q})$:

$$\Pi(\mathbf{u}(\mathbf{q}))=\tfrac{1}{2}\mathbf{u}^{\mathrm{T}}\mathbf{K}\,\mathbf{u}\,, \tag{7}$$

where $\mathbf{K}$ is the local stiffness matrix, which can be either constant or coordinate-dependent.

Virtual work $W$ of applied forces, such as gravity, is accounted in Eq. (5) for by expression

$$W(\mathbf{q})=\int_0^L \mathbf{r}(\mathbf{q})^{\mathrm{T}}\,\mu\mathbf{g}\,dx\,. \tag{8}$$

Finally, the equations of motion (5) can be written down in a matrix form as follows:

$$\mathbf{M}(\mathbf{q})\,\ddot{\mathbf{q}}+\mathbf{f}^{\mathrm{i}}(\dot{\mathbf{q}},\mathbf{q})+\mathbf{f}^{\mathrm{e}}(\mathbf{q})=\mathbf{f}^{\mathrm{a}}(\mathbf{q})\,, \tag{9}$$

See the detailed expressions in the Appendix 1.

## 3 SOLUTION PROCEDURES

The equations of motion of drill strings are normally stiff. Main sources of that are stiff forces such as forces in the connecting beams and contact forces between the drill strings and well bores. Contact interaction is simulated by a specialized *Circle-Cylinder* contact force

elements [1]. A force is considered stiff if its value significantly changes under small variations of relative positions and velocities of interacting bodies.

The implicit Park method with using approximated local Jacobian matrices of stiff forces is applied for numerical integration of equation of motions [2].

For the models created by the modal approach, parallel computations are implemented for multi-core processors. This allows effective simulating very long drill strings (up to several kilometers in length). For example, rotary drilling operation in the torque and drag analysis of drill string having six kilometers in length is simulated within five minutes CPU time using Intel® Core™ i7 processor 3GHz. The model includes 1 292 beams and 15 504 degrees of freedom. Computing such models in a single thread is practically impossible.

In the current version, the parallel calculations are not implemented for the models created by finite element method. However it is expected that calculation efficiency will be higher as compared with the modal approach because the number of degrees of freedom will decrease to a half.

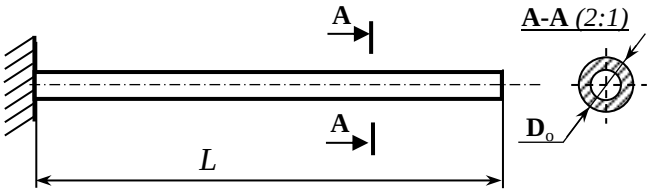


Figure 4. Outline of the cantilever beam.

Table 1.

Parameters of the beam used in the numerical tests.

| Parameter | Value | Comments |
|---|---|---|
| Geometry | | |
| $L$ | 3.0 M | Beam Length |
| $D_O$ | 0.08 M | Cross Section Outer Diameter |
| $D_I$ | 0.06 M | Cross Section Inner Diameter |
| Material Properties | | |
| $E$ | $2.1\times10^{11}$ N/m$^2$ | Young Modulus |
| $\nu$ | 0.3 | Poisson Ratio |
| $G$ | $7.692\times10^{10}$ N/m$^2$ | Shear Modulus |
| $P$ | 7800 kg/M$^3$ | Material Density |

## 4 TEST SIMULATION EXAMPLES

In the paper [1], the results of several tests which were carried out to verify the feasibilities of the modal approach are presented. The set of the tests includes the calculation of natural frequencies and modes of uniform beams, simulation of constrained buckling as well as static and vibration analysis of the real bottom hole assembly (BHA). All obtained results are very close to known theoretical solutions or well agree with the results calculated in Abaqus. In

this chapter, the comparison of the test results with uniform beam obtained by both proposed approaches is presented.

The outline of the cantilever beam is shown in figure 4. Its parameters used for numerical experiments are in table 1.

The models of each beam created by modal approach use only constrained modes. The modes are calculated for ten finite elements. Each beam has 12 degrees of freedom: 6 coordinates define the position and orientation of the local frames and 6 transformed modes to simulate flexibility. The linear and angular stiffness of the connecting force elements are $1\times10^{11}$ N/m and $1\times10^{11}$ Nm/rad.

Table 2.

The lowest natural frequency corresponding to the bending modes. Simulation results.

| № | Theor. Value, Hz | Number Of Beams / Fe | N Dof | Simulation Values, Hz | Error, % |
|---|---|---|---|---|---|
| 1 | 8.065 | 2 BEAM | 18 | 8.060 | -0.06 |
| | | 2 FE | 12 | 8.069 | 0.05 |
| | | 4 BEAM | 42 | 8.063 | -0.03 |
| | | 4 FE | 24 | 8.065 | 0.00 |
| | | 10 BEAM | 114 | 8.065 | 0.00 |
| | | 10 FE | 60 | 8.065 | 0.00 |
| 2 | 50.544 | 2 BEAM | 18 | 50.767 | 0.44 |
| | | 2 FE | 12 | 50.971 | 0.84 |
| | | 4 BEAM | 42 | 50.538 | -0.01 |
| | | 4 FE | 24 | 50.601 | 0.11 |
| | | 10 BEAM | 114 | 50.538 | -0.01 |
| | | 10 FE | 60 | 50.544 | 0.00 |
| 3 | 141.538 | 2 BEAM | 18 | 170.704 | 20.61 |
| | | 2 FE | 12 | 172.374 | 21.79 |
| | | 4 BEAM | 42 | 142.385 | 0.60 |
| | | 4 FE | 24 | 142.603 | 0.75 |
| | | 10 BEAM | 114 | 141.524 | -0.01 |
| | | 10 FE | 60 | 141.528 | -0.01 |

***Natural frequency and modes***

The results of calculating the lowest natural frequencies corresponding to the bending modes are presented in table 2. As we can see, the first and second frequencies are accurately calculated by all models. For accurate computation of the third frequency, two finite elements and two beams are not enough.

Note, that relative errors of the results obtained by models of both types are very close but finite element models include the numbers of degrees of freedom less than beams.

***Euler buckling simulation***

In accordance with the theoretical solution, a cantilever beam loses stability under axial

load when its value exceeds

$$F_1^{critical} = \left(\frac{\pi}{2L}\right)^2 EJ,$$

where $J$ is the geometrical moment of inertia of a cross-section of the beam.

Two approaches can be used for calculation of the critical force in «Universal Mechanism» software. These are the root locus approach and integration of equation of motion of the beam under increasing axial load. Note, that the first approach can be applied if boundary conditions do not change during buckling process. In order to exactly calculate the critical force using the second approach, a small disturbance is needed at the beginning time. To compute the critical force for Euler buckling of the beam, the root locus method is used. The critical force for the first shape is equal to 79 131 N.

The simulation results, obtained by different models are presented in tables 3 and 4. In addition to the used beam models connected via force element, the results for connecting by fixed joints are presented. These models give more accurate values for the critical force. But fixed joint are not widely used in UM for the simulation of real drill strings because of the parallel computations are currently not implemented for these connections.

Table 3.

The first critical force calculated by finite element models with the linear stiffness matrix.

| NUMBER OF FINITE ELEMENTS | $F_{CRITICAL,}$ N | *ERROR*, % |
|---|---|---|
| 1 | – | |
| 2 | 101 396 | 28.137 |
| 4 | 83 738 | 5.823 |
| 10 | 79 813 | 0.862 |

Table 4.

The first critical force calculated by finite element models with the nonlinear stiffness matrix.

| NUMBER OF FINITE ELEMENTS | $F_{CRITICAL,}$ N | *ERROR*, % |
|---|---|---|
| 1 | 79 725 | 0.751 |
| 2 | 79 179 | 0.061 |
| 4 | 79 141 | 0.013 |
| 10 | 79 141 | 0.013 |

It is clear that already two beams connected via joints and one finite element with nonlinear stiffness matrix give accurate values of the critical force. The results obtained by the models with two beams connected by force elements can be considered as acceptable ones for the engineering applications. Note that the real drill strings are not modeled by one beam. As a rule, they include several hundred of beams.

***Large deflection of a cantilever beam***

Another important static test, which is relevant to modeling of drill strings, is the large deflection static test. In Figure 5, a cantilever beam loaded its own weight marked by $q$ and a concentrated force $F$ is shown.

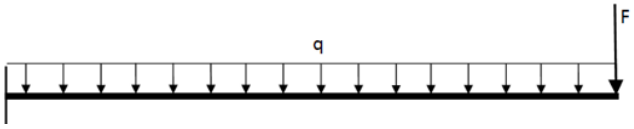


Figure 5. Simulation of static deflection of uniform

Material and cross-section parameters of the beam are taken as pointed out in Table 1, with exception of length parameter $L$, which is chosen in this case as $L$ = 20 m to achieve large displacements. The numerical simulation of the problem has been carried out using 2, 4, and 10 finite elements and beams. The loading conditions are chosen in such way that deflection due to own weight $q$ and one due to end-point force $F$ are of the same order of magnitude, as shown in Table 5 in the last row, where an exact reference solution is presented. The exact solution is obtained by numerical solving the nonlinear elastica differential equation in Maple software:

$$EI\frac{\mathrm{d}^2\varphi(s)}{\mathrm{d}s^2}+(F+q(L-s))\cos\varphi(s)=0,$$

$$\varphi(0)=0,\quad \frac{\mathrm{d}^2\varphi(L)}{\mathrm{d}s^2}=0.$$

where $\varphi(s)$ is the function of interest, the absolute rotation of the beam cross section. As soon as $\varphi(s)$ is determined from the latter equations, the deflection curve can be obtained as an integral, easily computed by the Maple software:

$$y(s)=\int_0^L \sin\varphi(\sigma)\,\mathrm{d}\sigma$$

Table 5.

Large static deflection of the end the long cantilever beam using finite element models, in meters

| N ELEM. | $F=1000$ N | | $Q=MG/L\approx$ 168 N/M | | $F$ AND $Q$ TOGETHER | |
|---|---|---|---|---|---|---|
| | LINEAR | NON LIN. | LINEAR | NON LIN. | LINEAR | NON LIN. |
| 2 | 8.15 | 8.11 | 10.36 | 10.33 | 14.29 | 14.25 |
| 4 | 7.89 | 7.86 | 9.75 | 9.70 | 13.24 | 13.16 |
| 10 | 7.79 | 7.79 | 9.52 | 9.49 | 12.86 | 12.64 |
| EXACT | | 7.77 | | 9.47 | | 12.77 |

The numerical results presented in Table 5 show the convergence of the numerical solution to the exact solution. Two modes of numerical solution were used: with employing the constant local stiffness matrix, and the non-linear local stiffness matrix **K**, see appendix.

The results for the same test obtained by the beam models with modal approach are presented in Table 6. The maximum error observed for the complex loading by using two beams is equal to 3.78%. All other results are practically exact.

Table 6.

Large static deflection of a long cantilever beam obtained by modal approach, in meters.

| N BEAMS | $F = 1000$ N | $Q = MG/L \approx 168$ N/M | $F$ AND $Q$ TOGETHER |
|---|---|---|---|
| 2 | 7.86 | 9.74 | 13.25 |
| 4 | 7.79 | 9.53 | 12.87 |
| 10 | 7.77 | 9.48 | 12.78 |
| EXACT | 7.77 | 9.47 | 12.77 |

## CONCLUSIONS

A modification of a nonlinear beam finite element is proposed for drill string analysis based on methods of multibody system dynamics is considered. The test results are given for eigenvalue analysis, for static and dynamic problems. The results are compared with analytical values where it is possible; if not, the results are compared to another finite element method using a modal approach. Both types of models give close results in test calculations of natural frequencies and modes, critical buckling forces and static deflections. The results well agree with theoretical ones. However, the number of degrees of freedom of finite element models is decreased to a half as compared with modal ones.

All considered methods and algorithms are implemented in specialized software developed on the base of 'Universal Mechanism' software package. It allows simulating dynamics of very long drill strings using models created by the modal approach.

Parallel computations for the finite element models of drill strings are currently not implemented. However, it is expected that this approach will be more efficient because a lesser amount of DOFs is used as compared to modal approach.

## ACKNOWLEDGMENTS

The authors would like to acknowledge the support of Weatherford Ltd. and Russian Foundation for Basic Researches, grant 14-01-00662-a.

## REFERENCES

[1] D. Pogorelov, G. Mikheev, N. Lysikov, L. Ring, R. Gandikota and N. Abedrabbo, A Multibody System Approach to Drill String Dynamics Modeling, *2012 Proceedings of the ASME 11th Biennial Conference on Engineering Systems Design and Analysis (ESDA2012)*, Volume 4, ISBN No: 978-0-7918-4487-8, pp. 53-62, 2012.

[2] D. Yu. Pogorelov. Jacobian matrices of the motion equations of a system of bodies. *Journal of Computer and Systems Sciences International*, 46, Nr. 4, 563–577, 2007.

[3] «Universal Mechanism», www.universalmechanism.com

[4] S. Timoshenko, D.H. Young, W. Weaver, Jr. Vibration problems in engineering, John Wiley & Sons, Inc, 1974.

[5] Shabana A.A. Flexible multibody dynamics: review of past and recent developments // Multibody System Dynamics 1, 1997, 189-222.
[6] Simo J.C. A finite strain beam formulation. The three-dimensional dynamic problem, Part I // Computer Methods in Applied Mechanics and Engineering 49, 1985, 55-70.

## APPENDIX. DERIVATION OF EQUATIONS OF MOTION OF THE NONLINEAR FINITE ELEMENT.

Equations of motion (9) of a nonlinear beam finite element contain the following main terms

$$\mathbf{M}(\mathbf{q}) = \frac{\partial^2 T}{\partial\dot{\mathbf{q}}\partial\dot{\mathbf{q}}} = \int_0^L \mu \mathbf{S}^{\mathrm{T}}\mathbf{S}\,\mathrm{d}x + \mathbf{M}^{\mathrm{t}}(\mathbf{q}), \tag{10}$$

$$\mathbf{f}^{\mathrm{i}}(\dot{\mathbf{q}},\mathbf{q}) = \int_0^L \mu \mathbf{S}^{\mathrm{T}}\dot{\mathbf{S}}\,\mathrm{d}x\,\dot{\mathbf{q}} + \mathbf{k}^{\mathrm{i}_{\mathrm{t}}}(\dot{\mathbf{q}},\mathbf{q}), \tag{11}$$

$$\mathbf{f}^{\mathrm{e}}(\mathbf{q}) = \frac{\partial \Pi}{\partial \mathbf{q}} = \mathbf{U}(\mathbf{q})^{\mathrm{T}}\mathbf{K}\,\mathbf{u}(\mathbf{q}), \tag{12}$$

$$\mathbf{f}^{\mathrm{a}}(\mathbf{q}) = \frac{\partial W}{\partial \mathbf{q}} = \int_0^L \mu \mathbf{S}(\mathbf{q})^{\mathrm{T}}\,\mathrm{d}x\,\mathbf{g}, \tag{13}$$

Value $\mu$ is the density of the beam material per unit length. $\mathbf{S} = \partial\mathbf{r}/\partial\mathbf{q}$ and $\mathbf{U} = \partial\mathbf{u}/\partial\mathbf{q}$ are Jacobian matrices:

$$\mathbf{S}(\mathbf{q},x) \underset{\text{Eq.(4)}}{=} \underbrace{[\mathbf{I} \quad -\mathbf{A}_1\tilde{\boldsymbol{\rho}}(\mathbf{q},x)\mathbf{A}_1^{\mathrm{T}}\mathbf{B}_1 \quad \mathbf{O} \quad \mathbf{O}]}_{\mathbf{S}_1(\mathbf{q},x)} + \mathbf{A}_1\mathbf{N}(x)\mathbf{U}(\mathbf{q}) \tag{14}$$

$$\mathbf{U}(\mathbf{q}) = \frac{\partial \mathbf{u}}{\partial \mathbf{q}} \overset{\text{Eq.(2)}}{=} \begin{bmatrix} -\mathbf{A}_1^{\mathrm{T}} & \mathbf{A}_1^{\mathrm{T}}\tilde{\{}\mathbf{r}_2 - \mathbf{r}_1\}\mathbf{B}_1 & \mathbf{A}_1^{\mathrm{T}} & \mathbf{O} \\ \mathbf{O} & -\mathbf{A}_1^{\mathrm{T}}\mathbf{B}_1 & \mathbf{O} & \mathbf{A}_1^{\mathrm{T}}\mathbf{B}_2 \end{bmatrix}, \tag{15}$$

where $\mathbf{B}_1$ and $\mathbf{B}_2$ are Jacobian matrices of angular velocity w.r.t. generalized velocities,

$$\mathbf{A}_i = \begin{bmatrix} c_{\beta_i}c_{\gamma_i} & -c_{\beta_i}s_{\gamma_i} & s_{\beta_i} \\ s_{\alpha_i}s_{\beta_i}c_{\gamma_i}+c_{\alpha_i}s_{\gamma_i} & c_{\alpha_i}c_{\gamma_i}-s_{\alpha_i}s_{\beta_i}s_{\gamma_i} & -s_{\alpha_i}c_{\beta_i} \\ s_{\alpha_i}s_{\gamma_i}-c_{\alpha_i}s_{\beta_i}c_{\gamma_i} & s_{\alpha_i}c_{\gamma_i}+c_{\alpha_i}s_{\beta_i}s_{\gamma_i} & c_{\alpha_i}c_{\beta_i} \end{bmatrix}, \tag{16}$$

$$\mathbf{B}_i = \frac{\partial \boldsymbol{\omega}_i}{\partial \dot{\boldsymbol{\varphi}}_i} = \begin{bmatrix} 1 & 0 & 0 \\ 0 & \cos\alpha_i & \sin\alpha_i \\ \sin\beta_i & -\sin\alpha_i\cos\beta_i & \cos\alpha_i\cos\beta_i \end{bmatrix} \text{ for Cardan angles}$$

In Eq. (14) and below, zero and unity 3×3 matrices are also used: $\mathbf{O} = \mathbf{O}_{3\times3}$, $\mathbf{I} = \mathbf{diag}(1,1,1)$.

Torsional component $\mathbf{M}^{\mathrm{t}}$ of the mass matrix in Eq. (10) has the following form:

$$\mathbf{M}(\mathbf{q})^{\mathrm{t}} \underset{\text{Eq.(?)}}{\overset{\text{Eq.(6)}}{=}} \mathbf{B}_1^{\mathrm{T}}\mathbf{A}_1\mathbf{J}^{\mathrm{t}}\mathbf{A}_1^{\mathrm{T}}\mathbf{B}_1 + \mathbf{B}_2^{\mathrm{T}}\mathbf{A}_2\mathbf{J}^{\mathrm{t}}\mathbf{A}_2^{\mathrm{T}}\mathbf{B}_2$$

where $\mathbf{J}^{\mathrm{t}} = \begin{bmatrix} J_{11} & 0 & 0 \\ 0 & 0 & 0 \\ 0 & 0 & 0 \end{bmatrix}$ is the tensor of inertia around local axis x, $J_{11} = \frac{1}{2}\frac{m}{A}J_x$, and $J_x$ is the torsional area moment of the beam.

Detailed expression for the mass matrix in Eq. (10) is obtained by direct computation:

$$\int_0^L \mu \mathbf{S}^{\mathrm{T}}\mathbf{S}\,\mathrm{d}x \overset{\text{Eq.(6)}}{=} \underbrace{\int_0^L \mu \mathbf{S}_1^{\mathrm{T}}\mathbf{S}_1\mathrm{d}x}_{part\ 1} + \underbrace{\mathbf{U}^{\mathrm{T}}\int_0^L \mu \mathbf{N}^{\mathrm{T}}\mathbf{A}_1^{\mathrm{T}}\mathbf{S}_1\mathrm{d}x}_{part\ 2} + \underbrace{\mathbf{U}^{\mathrm{T}}[\int_0^L \mu \mathbf{N}^{\mathrm{T}}\mathbf{N}\mathrm{d}x]\mathbf{U}}_{part\ 3} + \underbrace{\int_0^L \mu \mathbf{S}_1^{\mathrm{T}}\mathbf{A}_1\mathbf{N}\mathrm{d}x\,\mathbf{U}}_{transpose\ of\ part\ 2} \tag{17}$$

It consists of three different parts, as shown in the latter formula. They are as follows:

$$\underbrace{\int_0^L \mu \mathbf{S}_1^{\mathrm{T}}\mathbf{S}_1\mathrm{d}x}_{part\ 1} \overset{\text{Eq.(6)}}{=} \left[\begin{array}{c|cc|c} m\mathbf{I} & -\mathbf{A}_1\tilde{\bar{\boldsymbol{\rho}}}\mathbf{A}_1^{\mathrm{T}}\mathbf{B}_1 & \mathbf{O} & \mathbf{O} \\ \mathbf{B}_1^{\mathrm{T}}\mathbf{A}_1\tilde{\bar{\boldsymbol{\rho}}}\mathbf{A}_1^{\mathrm{T}} & \mathbf{B}_1^{\mathrm{T}}\mathbf{A}_1\mathbf{J}_{\boldsymbol{\rho}}\mathbf{A}_1^{\mathrm{T}}\mathbf{B}_1 & \mathbf{O} & \mathbf{O} \\ \mathbf{O} & \mathbf{O} & \mathbf{O} & \mathbf{O} \\ \mathbf{O} & \mathbf{O} & \mathbf{O} & \mathbf{O} \end{array}\right], \tag{18}$$

$$\mathbf{U}^{\mathrm{T}}\int_0^L \mu \mathbf{N}^{\mathrm{T}}\mathbf{A}_1^{\mathrm{T}}\mathbf{S}_1\mathrm{d}x \overset{\text{Eq.(6)}}{=} \left[\begin{array}{c|cc|c} \mathbf{U}^{\mathrm{T}}\left[\bar{\mathbf{N}}^{\mathrm{T}}\mathbf{A}_1^{\mathrm{T}}\right. & \left.[\tilde{\bar{\boldsymbol{\rho}}}\mathbf{N}]^{\mathrm{T}}\mathbf{A}_1^{\mathrm{T}}\mathbf{B}_1\right. & \mathbf{O} & \left.\mathbf{O}\right] \end{array}\right] \tag{19}$$

*part* 3: see Eq. (21) below.

Some terms after integration in Eq. (18) and (19) appear as follows:

$$\bar{\boldsymbol{\rho}} = \mu\int_0^L \boldsymbol{\rho}\mathrm{d}x \overset{\text{Eq.(3)}}{=} \underbrace{\int_0^L \mu\boldsymbol{\rho}_*\mathrm{d}x}_{\bar{\boldsymbol{\rho}}_*} + \underbrace{\int_0^L \mu\mathbf{N}\mathrm{d}x}_{\bar{\mathbf{N}}}\mathbf{u} = \bar{\boldsymbol{\rho}}_* + \bar{\mathbf{N}}\mathbf{u},$$

$$\bar{\boldsymbol{\rho}}_* = \{\tfrac{mL}{2},\,0,\,0\}^{\mathrm{T}}, \quad \bar{\mathbf{N}} = \int_0^L \mu\mathbf{N}\mathrm{d}x = \begin{bmatrix} \frac{m}{2} & 0 & 0 & 0 & 0 & 0 \\ 0 & \frac{m}{2} & 0 & 0 & 0 & \frac{-mL}{12} \\ 0 & 0 & \frac{m}{2} & 0 & \frac{mL}{12} & 0 \end{bmatrix}$$

Tensor of inertia $\mathbf{J}_{\boldsymbol{\rho}}$ in local frame depends on local coordinates $\mathbf{u}$:

$$\begin{aligned} \mathbf{J}_{\boldsymbol{\rho}} &= -\mu\int_0^L \tilde{\boldsymbol{\rho}}\tilde{\boldsymbol{\rho}}\mathrm{d}x = -\mu\int_0^L [\tilde{\boldsymbol{\rho}}_* + \tilde{\{}\mathbf{Nu}\}][\tilde{\boldsymbol{\rho}}_* + \tilde{\{}\mathbf{Nu}\}]\mathrm{d}x \\ &= -\mu\int_0^L [\tilde{\boldsymbol{\rho}}_*\tilde{\boldsymbol{\rho}}_* + \tilde{\{}\mathbf{Nu}\}\tilde{\mathbf{i}}x + \tilde{\mathbf{i}}x\tilde{\{}\mathbf{Nu}\} + \tilde{\{}\mathbf{Nu}\}\,\tilde{\{}\mathbf{Nu}\}]\mathrm{d}x \\ &= \mathbf{J}_{\boldsymbol{\rho}^*} - 2\mathbf{sym}[\,\tilde{\{}\,\bar{[}\mathbf{N}x]\mathbf{u}\}\tilde{\mathbf{i}}\,] - \bar{[}\mathbf{N}\mathbf{u}\mathbf{u}^{\mathrm{T}}\mathbf{N}^{\mathrm{T}}] + (\mathbf{u}^{\mathrm{T}}\bar{[}\mathbf{N}^{\mathrm{T}}\mathbf{N}]\mathbf{u})\mathbf{I} \end{aligned} \tag{20}$$

where

$$\bar{[}\mathbf{N}x] = \int_0^L \mu\,\mathbf{N}(x)x\,\mathrm{d}x = \begin{bmatrix} \frac{mL}{6} & 0 & 0 & 0 & 0 & 0 \\ 0 & \frac{7mL}{20} & 0 & 0 & 0 & \frac{-mL^2}{20} \\ 0 & 0 & \frac{7mL}{20} & 0 & \frac{mL^2}{20} & 0 \end{bmatrix}$$

and $\bar{[}\tilde{\boldsymbol{\rho}}\mathbf{N}] = \int_0^L \mu\tilde{\boldsymbol{\rho}}\mathbf{N}\mathrm{d}x = \int_0^L \mu[\tilde{\boldsymbol{\rho}}_*\mathbf{N} + \tilde{\{}\mathbf{Nu}\}\mathbf{N}]\mathrm{d}x = \int_0^L \mu[\tilde{\mathbf{i}}x\mathbf{N} + \tilde{\{}\mathbf{Nu}\}\mathbf{N}]\mathrm{d}x = \tilde{\mathbf{i}}\,\bar{[}\mathbf{N}x] + \bar{[}\tilde{\{}\mathbf{Nu}\}\mathbf{N}]$

$$\bar{[}\tilde{\{}\mathbf{Nu}\}\mathbf{N}] = \int_0^L \mu\tilde{\{}\mathbf{Nu}\}\mathbf{N}\mathrm{d}x = m\begin{bmatrix} 0 & \frac{78u_3+11Lu_5}{-210} & \frac{78u_2-11Lu_6}{210} & 0 & \frac{11Lu_2-2L^2u_6}{210} & \frac{11Lu_3+2L^2u_5}{210} \\ \frac{7u_3+Lu_5}{20} & 0 & \frac{-7u_1}{20} & 0 & \frac{-Lu_1}{20} & 0 \\ \frac{Lu_6-7u_2}{20} & \frac{7u_1}{20} & 0 & 0 & 0 & \frac{-Lu_1}{20} \end{bmatrix}$$

An integral of squared shape function matrix produces the local mass matrix, used in Eq. (17):

$$\bar{[}\mathbf{N}^{\mathrm{T}}\mathbf{N}] = \underbrace{\int_0^L \mu \mathbf{N}^{\mathrm{T}}\mathbf{N}\mathrm{d}x}_{\mathrm{local\,mass\,matr.}} = \frac{m}{420}\begin{bmatrix} 140 & \mathrm{o} & \mathrm{o} & \mathrm{o} & \mathrm{o} & \mathrm{o} \\ \mathrm{o} & 156 & \mathrm{o} & \mathrm{o} & \mathrm{o} & 22L \\ \mathrm{o} & \mathrm{o} & 156 & \mathrm{o} & -22L & \mathrm{o} \\ \mathrm{o} & \mathrm{o} & \mathrm{o} & \mathrm{o} & \mathrm{o} & \mathrm{o} \\ \mathrm{o} & \mathrm{o} & -22L & \mathrm{o} & 4L^2 & \mathrm{o} \\ \mathrm{o} & 22L & \mathrm{o} & \mathrm{o} & \mathrm{o} & 4L^2 \end{bmatrix} \tag{21}$$

Note that the torsional inertia term [4,4] is equal to zero here since the torsional inertia is computed separately, see Eq. (10).

The last term needed above in Eq. (20) is $\bar{[}\mathbf{N}\mathbf{u}\mathbf{u}^{\mathrm{T}}\mathbf{N}^{\mathrm{T}}]$, which is computed as follows:

$$\bar{[}\mathbf{N}\mathbf{V}\mathbf{N}^{\mathrm{T}}] = \int_0^L \mu \mathbf{N}\mathbf{V}\mathbf{N}^{\mathrm{T}}\mathrm{d}x = m\begin{bmatrix} \frac{v_{11}}{3} & \frac{7v_{12}-Lv_{16}}{20} & \frac{7v_{13}+Lv_{15}}{20} \\ \frac{7v_{21}-Lv_{61}}{20} & \frac{78v_{22}-11L(v_{62}+v_{26})+2L^2v_{66}}{210} & \frac{78v_{23}-11Lv_{63}+11Lv_{25}+2L^2v_{65}}{210} \\ \frac{7v_{31}+Lv_{51}}{20} & \frac{78v_{32}-11Lv_{36}+11Lv_{52}+2L^2v_{56}}{210} & \frac{78v_{33}+11L(v_{53}+v_{35})+2L^2v_{55}}{210} \end{bmatrix}$$

(term $\mathbf{u}\mathbf{u}^{\mathrm{T}}$ is given in a general form as a non-symmetric 6×6 matrix $\mathbf{V} = [v_{ij}]$ needed below in Eq. **Ошибка! Источник ссылки не найден.**).

*Evaluation of inertia forces*

Vector of generalized inertia forces (11) contains acceleration term $\dot{\mathbf{S}}\dot{\mathbf{q}}$, which is the sum of the centripetal, Coriolis and relative accelerations of a beam's particle:

$$\dot{\mathbf{S}}\dot{\mathbf{q}} = \mathbf{a}'' = \underbrace{\tilde{\boldsymbol{\omega}}_1\tilde{\boldsymbol{\omega}}_1\mathbf{A}_1\boldsymbol{\rho}}_{\mathrm{centripetal\,acc.}} + \underbrace{2\tilde{\boldsymbol{\omega}}_1\mathbf{A}_1\dot{\boldsymbol{\rho}}}_{\mathrm{Coriolis\,acc.}} + \underbrace{\mathbf{A}_1\mathbf{N}\dot{\mathbf{U}}\dot{\mathbf{q}}}_{\mathrm{relative\,acc.}}$$

That is why the first term in Eq. (11) has the following detailization:

$$\mathbf{f}^{\mathrm{i}_1} = \int_0^L \mu \mathbf{S}^{\mathrm{T}}\mathbf{a}''\mathrm{d}x \overset{\mathrm{Eq.(14)}}{=} \int_0^L \mu[\mathbf{S}_1^{\mathrm{T}} + \mathbf{U}^{\mathrm{T}}\mathbf{N}^{\mathrm{T}}\mathbf{A}_1^{\mathrm{T}}][\tilde{\boldsymbol{\omega}}_1\tilde{\boldsymbol{\omega}}_1\mathbf{A}_1\boldsymbol{\rho} + 2\tilde{\boldsymbol{\omega}}_1\mathbf{A}_1\mathbf{N}\dot{\mathbf{u}} + \mathbf{A}_1\mathbf{N}\dot{\mathbf{U}}\dot{\mathbf{q}}]\mathrm{d}x \tag{22}$$

Value of $\mathbf{S}^{\mathrm{T}}$ has been already obtained above in parts; in Eq. (18), (19) they are marked by dotted lines, thus Eq. (22) takes the form

$$\mathbf{f}^{\mathrm{i}_1} = \int_0^L \mu \mathbf{S}_1^{\mathrm{T}}\mathbf{a}''\mathrm{d}x + \mathbf{U}^{\mathrm{T}}\int_0^L \mathbf{N}^{\mathrm{T}}\mathbf{A}_1^{\mathrm{T}}\mathbf{a}''\mathrm{d}x = \left\{\begin{array}{c} \tilde{\boldsymbol{\omega}}_1\tilde{\boldsymbol{\omega}}_1\mathbf{A}_1\bar{\boldsymbol{\rho}} + 2\tilde{\boldsymbol{\omega}}_1\mathbf{A}_1\bar{\mathbf{N}}\dot{\mathbf{u}} + \mathbf{A}_1\bar{\mathbf{N}}\dot{\mathbf{U}}\dot{\mathbf{q}} \\ \mathbf{B}_1^{\mathrm{T}}\tilde{\boldsymbol{\omega}}_1\mathbf{J}_{\boldsymbol{\rho}}^{(0)}\boldsymbol{\omega}_1 - 2\mathbf{B}_1^{\mathrm{T}}\mathbf{A}_1\bar{[}\tilde{\boldsymbol{\rho}}\tilde{\{}\mathbf{N}\dot{\mathbf{u}}\}]\boldsymbol{\omega}_1^{(1)} + \mathbf{B}_1^{\mathrm{T}}\mathbf{A}_1\bar{[}\tilde{\boldsymbol{\rho}}\mathbf{N}]\dot{\mathbf{U}}\dot{\mathbf{q}} \\ \mathbf{o} \\ \mathbf{o} \end{array}\right\} + \tag{23}$$

$$+ \mathbf{U}^{\mathrm{T}}\left[\tilde{\{}\mathbf{N}^{\mathrm{T}}\mathbf{A}_1^{\mathrm{T}}\tilde{\boldsymbol{\omega}}_1\tilde{\boldsymbol{\omega}}_1\mathbf{A}_1\boldsymbol{\rho}\} - 2\bar{[}\mathbf{N}^{\mathrm{T}}\tilde{\{}\mathbf{N}\dot{\mathbf{u}}\}]\boldsymbol{\omega}_1^{(1)} + \bar{[}\mathbf{N}^{\mathrm{T}}\mathbf{N}]\dot{\mathbf{U}}\dot{\mathbf{q}}\right]$$

There are two new terms in the expression to calculate, $\bar{[}\tilde{\boldsymbol{\rho}}\tilde{\{}\mathbf{N}\dot{\mathbf{u}}\}]$ and $\bar{\{}\mathbf{N}^{\mathrm{T}}\mathbf{A}_1^{\mathrm{T}}\tilde{\boldsymbol{\omega}}_1\tilde{\boldsymbol{\omega}}_1\mathbf{A}_1\boldsymbol{\rho}\}$ (skipped due to limitation of the paper size).